Chapter 7

Relaxation oscillations and Noise Analysis

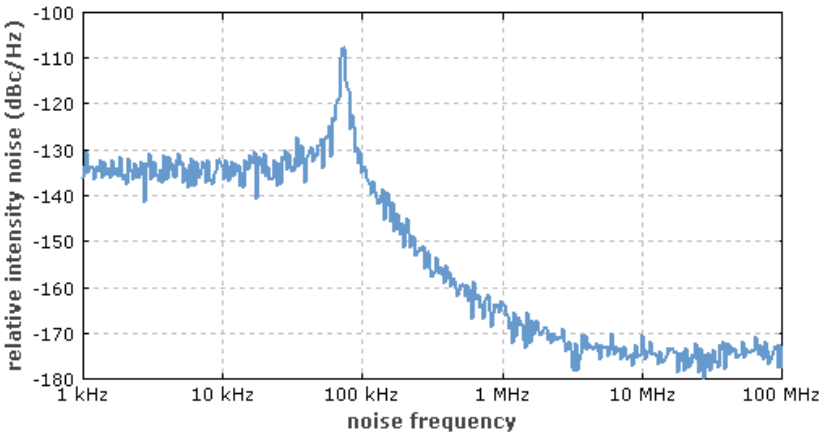

Figure 7.1: Relative intensity noise spectrum of a 1064-?nm Nd:YAG laser with 100 mW

7.1 Mathematical description of Noise [1]

The frequency and amplitude of even the most advanced oscillators are not really constant in time, but fluctuate. In the previous chapter we have analyzed the situation where these quantities were modulated in a strictly deterministic way. The harmonic modulation of the amplitude of an oscillation was found to lead to discrete sideband frequencies whereas the exponential temporal decay of the amplitude resulted in a continuous band of frequencies. In both cases, for any instant in the past or in the future one was able to predict the exact value of the instantaneous amplitude, frequency and the phase. For real oscillators, however, a large variety of physical processes that are not under control can affect these quantities in a complicated way. As a result, the amplitude, phase or frequency of any oscillator will fluctuate in an irregular way that in general can no longer be represented by an analytic function of time. These unwanted fluctuations are often referred to as noise or jitter. To describe these fluctuations, statistical measures have to be applied. The characterization of frequency standards in terms of statistical quantities nevertheless allows one to select the most suitable standard or to infer information about possible sources that degrade the performance of the standard.

For frequency standards one deals in general with the best available oscillators where often the statistical modulations of amplitude and phase are small. Consequently, one uses a model of the

[1] Chapter 3 (Page 47-68) - Frequency Standards Basics and Applications - Fritz Riehle - WILEY-VCH Verlag GmbH & Co. KGaA, 2004

oscillator where the instantaneous output signal of the oscillator is written as

$$U(t) = [U_0 + \Delta U(t)] \cos(2\pi\nu_0 t + \phi(t)) \tag{7.1.1}$$

The quantity $U(t)$ may represent, e.g., the signal from a quartz oscillator or the electric field of an oscillator in the microwave or optical domain. $\Delta U0(t)$ represents random rather than deterministic amplitude fluctuations around U_0. Similarly, the fluctuations $\phi(t)$ of the phase result from a random process. In (7.1.1) it is furthermore assumed that the fluctuations of the phase and amplitude are orthogonal meaning that no amplitude fluctuations are transferred to phase fluctuations and vice versa. To compare frequency standards operating at different frequencies ν_0 it is helpful to define the normalized phase fluctuations

$$x(t) \equiv \frac{\phi(t)}{2\pi\nu_0} \tag{7.1.2}$$

which are sometimes referred to as the phase time. Similarly, rather than using the fluctuations of the instantaneous frequency itself, the instantaneous fractional (or normalized) frequency deviation

$$y(t) \equiv \frac{\Delta\nu(t)}{\nu_0} = \frac{dx(t)}{dt} \tag{7.1.3}$$

is defined where $\Delta\nu(t) \equiv \frac{1}{2\pi}\frac{d\phi(t)}{dt}$ has been utilized to derive the latter equation.

7.1.1 Time-domain Description of Frequency Fluctuations

Consider the time sequence of a fluctuating quantity measured as a continuous function $y(t)$ (Fig. 7.2 a) or as series of discrete readings y_i (Fig. 3.1 b). The latter may be obtained, e.g., if the mea-

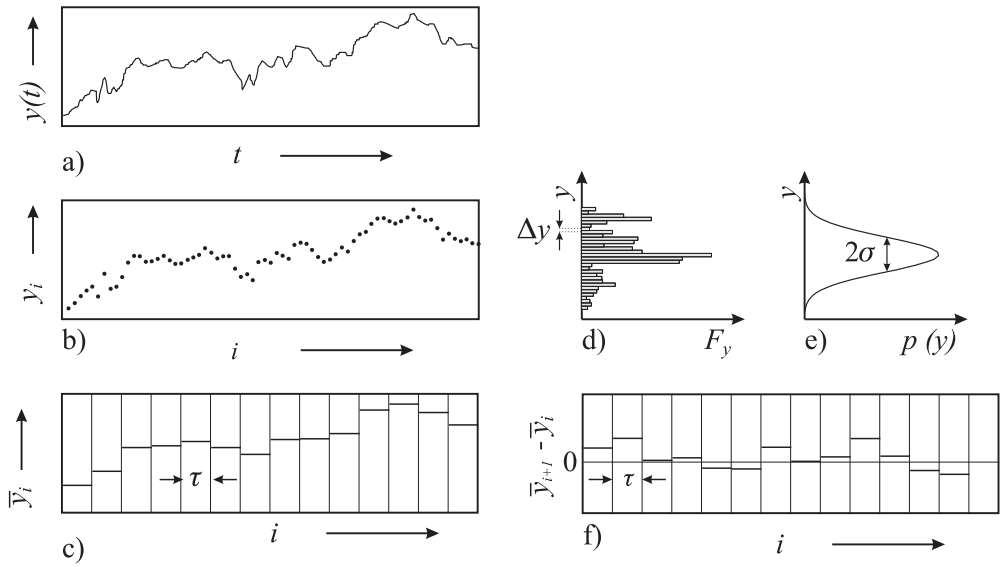

Figure 7.2: a) Continuous time sequence $y(t)$. b) Discrete time series y_i of a fluctuating quantity. c) Consecutive mean values of $y(t)$ (see Fig. 7.2 a) where the values $\overline{y_i}$ are taken during a duration τ. d) Histogram F_y corresponding to the distribution of y in the bin size Δy. e) Corresponding Gaussian probability density $p(y)$. f) $\overline{y}_{i+1} - \overline{y}_i$ used to compute the Allan variance according to (3.13).

surement of $y(t)$ was performed by using a frequency counter. As a result the continuous function $y(t)$ is reduced to a discrete series of consecutive measurements averaged over the measurement time τ

$$\overline{y}_i = \frac{1}{\tau}\int_{t_i}^{t_i+\tau} y(t)dt \tag{7.1.4}$$

(Fig. 7.2 c), referred to as the normalized frequency deviation averaged over the duration τ . As repeated measurements of y_i in general differ from each other (see Fig. 7.2 b), we recall in the

following the statistical means usually employed to characterize such a data set. It is well known that the mean value and the square of the experimental standard deviation are

$$\overline{y} = \frac{1}{N}\sum_{i=1}^{N} y_i \tag{7.1.5}$$

and

$$s_y^2 = \frac{1}{N-1}\sum_{i=1}^{N}(y_i - \overline{y})^2 = \frac{1}{N-1}\left[\sum_{i=1}^{N} y_i^2 - \frac{1}{N}\Big(\sum_{i=1}^{N} y_i\Big)^2\right] \tag{7.1.6}$$

respectively. The standard deviation of the mean is

$$s_{\overline{y}} = \frac{s_y}{\sqrt{N}} \tag{7.1.7}$$

s_y is a measure of the width of the histogram F_y (see Fig. 7.2 d) where the values of $y(t)$ (or y_i) have been grouped into bins of width Δy as a function of $y(t)$.

Often the fluctuations of $y(t)$ are thought to result from a statistical process. If the process causing the fluctuations of $y(t)$ is stationary,[2] according to the central-limit theorem of probability theory one expects that for $T \to \infty$, Fy evolves into a Gaussian probability density

$$p(y) = \frac{1}{\sigma\sqrt{2\pi}} \exp\left(-\frac{(y-\overline{y})^2}{2\sigma^2}\right) \tag{7.1.8}$$

(Fig. 7.2 d) with variance σ^2. The statistical process is characterized by the expectation value

$$\langle y\rangle \equiv \int_{-\infty}^{+\infty} y p(y) dy \tag{7.1.9}$$

and the variance

$$\sigma^2 = \int_{-\infty}^{+\infty} (y - \langle y\rangle)^2 p(y) dy \tag{7.1.10}$$

Using the notation of (7.1.9), (7.1.10) can be written as

$$\sigma^2 = \langle (y - \langle y\rangle)^2\rangle = \langle y^2 - 2y\langle y\rangle + \langle y\rangle^2\rangle = \langle y^2\rangle - \langle y\rangle^2 \tag{7.1.11}$$

The expectation value (7.1.9) and variance (7.1.10) of a statistical process can be only estimated from the measured finite sequence of the fluctuating quantity in such a way that the mean value (7.1.5) is an estimate for the expectation value $\langle y\rangle$ of the Gaussian process and the square of the standard deviation (7.1.6) is an estimate of its variance σ^2.

Besides defining mean value and standard deviation from consecutive measurements of, e.g., the frequency of a single oscillator, analogously, the mean value and standard deviation can be defined as a statistical average for a sample of identical oscillators. For a stationary process such a sample average is independent of the chosen time of the measurement. For an ergodic process,[3] σ^2 can be estimated either from the time average or from the sample average.[4]

The use of the statistical tools of mean value and standard deviation meets with difficulties if applied to fluctuating quantities with correlations. This can be seen if one divides the times series of Fig. 7.2 a) into equidistant intervals like in Fig. 7.2 c). A quick look reveals that the data of Fig. 7.2 a) or b) within each subset scatter much less than the data within the total interval.

[2] A statistical process is called stationary if the statistical measures describing the process, e.g., the mean value or the variance, are time independent.

[3] A process where the average over an infinite number of samples is identical to the infinite time average ($\langle y\rangle = \overline{y}$) is referred to as an ergodic process.

[4] Stationarity and ergodicity are mathematical properties that are often assigned to the statistical processes used to model the fluctuations of real frequency standards. As a result of the limited time available for any measurements and the limited number of identical frequency standards at hand these properties cannot be proven but merely represent reasonable assumptions. Care has to be taken when the results derived on these assumptions are applied to practical cases. During their lifetimes, e.g., frequency standards may become more "noisy" and stationarity may not be granted over this time.

The corresponding experimental standard deviations (7.1.6) calculated within each sub-interval in general are much smaller than the one calculated from the entire data set. This indicates that the adjacent data points are not independent of each other but are somehow correlated. Consequently, the standard deviation of the mean is not reduced by $1/\sqrt{N}$(see (7.1.7)) for N as would be the case for uncorrelated data. Thus, the determination of standard deviations from different subsets of the data can be used to get information about the existence of correlations. It has to be pointed out that the statistics of a fluctuating quantity with correlations can sometimes be well described by a Gaussian distribution and, hence, the lack of this property cannot be used to identify correlations.

7.1.2 Allan Variance

To make a meaningful estimate of the statistical process in the presence of correlations one has to specify the number N of measurements (samples), the measuring time τ of a single sample and the time T between consecutive measurements which may differ from τ by the dead time $T - \tau$ (see Fig. 7.3). After having done this one can readily define a so-called N-sample variance for this

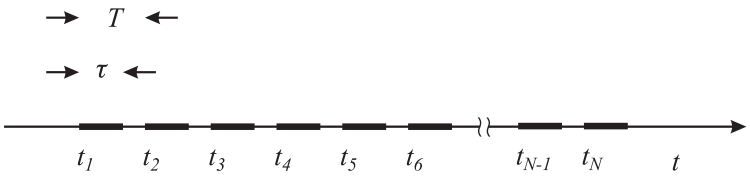

Figure 7.3: Measurement cycle.

data set in analogy to (7.1.6) as[5]

$$\sigma^2(N,T,\tau) = \frac{1}{N-1}\sum_{i=1}^{N}\left(\overline{y}_i - \frac{1}{N}\sum_{i=1}^{N}\overline{y}_i\right)^2 \tag{7.1.12}$$

for a given number N of samples and given values of T and τ (see Fig. 7.3). It is now generally agreed to follow a proposition made by Dave Allan and to select from all possible sample variances the expectation value of the so-called two-sample variance with $N = 2$ and $T = \tau$. Hence, this so-called Allan variance $\sigma_y^2(2,\tau,\tau)$ which is alternatively referred to as short-hand notation $\sigma_y^2(2,\tau)$ or $\sigma_y^2(\tau)$, is defined using (7.1.12) as

$$\boxed{\sigma^2(\tau) = \Big\langle \sum_{i=1}^{2}\left(\overline{y}_i - \frac{1}{2}\sum_{i=1}^{2}\overline{y}_i\right)^2 \Big\rangle = \frac{1}{2}\langle(\overline{y}_2 - \overline{y}_1)^2\rangle} \tag{7.1.13}$$

The Allan variance and its square root sometimes termed the Allan (standard) deviation is based on differences of adjacent frequency values rather than on frequency differences from the mean value, as is the "true" standard deviation.

Alternatively, the Allan variance can be determined from the phase deviation $\phi(t)$ or the normalized phase deviation $x(t)$. For a given measuring interval τ it follows from (7.1.3) that

$$\overline{y}_i = \frac{\overline{x}_{i+1} - \overline{x}_i}{\tau} \tag{7.1.14}$$

which after insertion into (7.1.13) gives

$$\sigma^2(\tau) = \frac{1}{2\tau^2}\Big\langle(\overline{x}_{i+2} - 2\overline{x}_{i+1} + \overline{x}_i)^2\Big\rangle \tag{7.1.15}$$

[5]To be more specific, there is more than one possible definition for the N sample variance. The various definitions differ by the pre-factor and each have their advantages for a particular type of noise.

7.1.3 Practical Determination of the Allan Variance

In the experiment the Allan variance of a particular oscillator 1 may be determined, e.g., from a beat note , i.e., the frequency difference with respect to a second oscillator 2 (reference oscillator) using a counter gated with the measuring time τ . According to the definition it has to be ensured that there is no dead time between two adjacent measurements. From the squared normalized frequency differences between two adjacent pairs ν_i and ν_{i+1} the mean value is computed and divided by 2 to give the Allan variance $\sigma^2_{y,tot}$ for the particular measuring time τ . To make a good approximation of the expectation value ($\langle\rangle$) of (7.1.13) a sufficiently large number of frequency differences has to be used. The procedure has to be repeated for the different times τ and may lead to Allan deviations such as the ones displayed in Fig. 7.4. In Fig. 7.4 the Allan deviations $\sigma_y(\tau)$ of various frequency standards and oscillators are compared with frequencies ranging from the microwave region to the optical regime.

In practice the Allan variance is determined in slightly different ways in order to allow for the minimum measurement time necessary to retrieve the full information required. The counter is set to the shortest gate time τ_0 where the Allan variance is to be determined and the frequency difference $\overline{y}_{i,\tau_0}$ between the oscillators is measured repeatedly and the data are stored making sure that no deadtime occurs during the data acquisition (see Fig. 7.4 a). To derive the data for longer times, e.g., $\tau = 3\tau_0$ the consecutive values of $\overline{y}_{1,\tau} = (\overline{y}_{1,\tau_0} + \overline{y}_{2,\tau_0} + \overline{y}_{3,\tau_0})/3$, $\overline{y}_{2,\tau} = (\overline{y}_{4,\tau_0} + \overline{y}_{5,\tau_0} + \overline{y}_{5,\tau_0})/3$, $\overline{y}_{3,\tau_0} = \cdots$ are determined in a post processing (Fig. 7.4 b) to estimate the Allan variance for the time $\tau = 3\tau_0$ and accordingly for all other times τ .

To make even better use of the stored data, roughly n times more values of $\overline{y}_{i,\tau=n\tau_0}$ can be obtained if the data processing is done in the way depicted in Fig. 7.4 c) where $\overline{y}_{1,\tau} = (\overline{y}_{1,\tau_0} + \overline{y}_{2,\tau_0} + \overline{y}_{3,\tau_0})/3$, $\overline{y}_{2,\tau} = (\overline{y}_{4,\tau_0} + \overline{y}_{5,\tau_0} + \overline{y}_{5,\tau_0})/3$, $\overline{y}_{3,\tau_0} = \cdots$ are taken

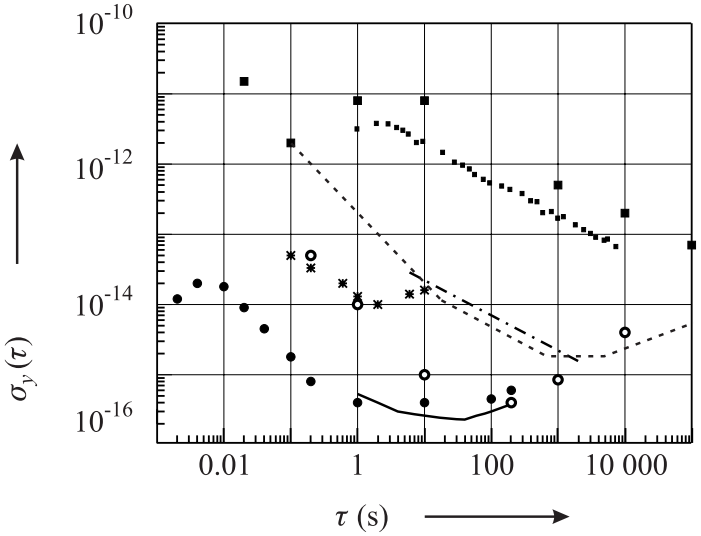

Figure 7.4: Allan deviation $\sigma_y(\tau)$ as a function of the measuring time τ for various highly stable oscillators used as frequency standards and discussed in this book: commercial cesium atomic clock (big squares, small squares), hydrogen maser (typical, dashed line), caesium fountain (dashed dotted line) , sapphire loaded cavity microwave oscillator (thick line) , superconducting-cavity stabilized microwave oscillator (open circles , laser stabilized to a FabryProt cavity (full circles), Ca stabilized laser (asterisks).

If the reference oscillator is known to be of superior stability with respect to the oscillator under test, the Allan variance is a measure of the instability of the latter one. If the Allan variance of two identical oscillators “1” and “2” is taken one is led to assume that both oscillators contribute equally to the instability and the measured Allan variance $\sigma_{y,tot}$ is attributed evenly to both

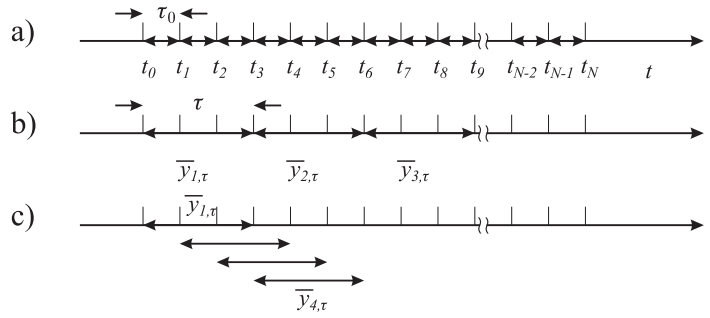

Figure 7.5: Alternative methods of calculating the Allan variance.

oscillators as follows

$$\sigma^2_{y,tot}(\tau) = \sigma^2_{y,1}(\tau) + \sigma^2_{y,2}(\tau) \qquad \text{and}$$
$$\sigma_{y,1}(\tau) = \sigma_{y,2}(\tau) = \frac{1}{\sqrt{2}}\sigma_{y,tot}(\tau) \tag{7.1.16}$$

The Allan variance $\sigma^2_y(\tau)$ is a useful time-domain measure of the frequency instability of an oscillator. It allows one to select the ideal oscillator for a particular application. As an example, consider the Allan variance of a typical hydrogen maser and one of the best frequency stabilized lasers shown in Fig. 7.4. The latter one has an optimum stability of $\sigma_y \leq 5\times10^{-16}$ for measurement times τ between 1 s and 100 s whereas the former one reaches its optimum frequency stability at one to several hours. In the plot of $\sigma_y(\tau)$ one often can identify regions where the frequency instability of a particular frequency standard follows a well defined power law. We will see in Section 7.1.4 that a linear drift leads to an Allan deviation proportional to τ . The relationship between the τ^{-1} and $\tau^{-1/2}$ dependencies recognized, e.g., in the plot of the hydrogen maser (Fig. 7.4) and the underlying noise processes will be discussed. Besides stochastic fluctuations, deterministic variations of the frequency of a given oscillator have a profound impact on the measured Allan variance. In the following we will investigate two important cases, a linear frequency drift and an harmonic frequency modulation.

7.1.4 Influence of a Linear Frequency Drift

Consider an oscillator whose normalized frequency shows a linear drift $y(t) = at$ where a is the slope of the drift. With $\overline{y}_1 = [at_0 + a(t_0 + \tau)]/2$ and $\overline{y}_2 = [a(t_0 + \tau) + a(t_0 + 2\tau)]/2$ one calculates from (7.1.13)

$$\sigma_y(\tau) = \langle a\tau/\sqrt{2}\rangle = \frac{a}{\sqrt{2}}\tau \qquad \text{for linear frequency drift.} \tag{7.1.17}$$

Hence, a linear frequency drift leads to an Allan deviation that linearly increases with measuring time τ .

7.1.5 Influence of an Harmonic Modulation

Next we consider an oscillator whose frequency is modulated with a sinusoidal modulation frequency fm as[6]

$$y(t) = \frac{\Delta\nu_0}{\nu_0}\sin(2\pi f_m t) \tag{7.1.18}$$

Calculating (7.1.13) by use of (7.1.18) leads to

$$\sigma_y(\tau) = \frac{\Delta\nu_0}{\nu_0}\frac{\sin(\pi f_m t)}{\pi f_m t} \qquad \text{for modulation with sinusoidal signal.} \tag{7.1.19}$$

[6]In this chapter modulation and Fourier frequencies are denoted by f rather than by ν to allow for better distinction with respect to the carrier frequency.

From (7.1.19) one finds that the influence of the frequency modulation on the Allan deviation becomes zero for $\tau = 1/f_m$, i.e., when τ equals the modulation period $1/f_m$ or one of its harmonics, where the influence of the modulation is averaged to zero. It is maximal for $\tau \approx n/(2f_m)$ with n an odd integer.

7.1.6 The Wiener-Khintchine Theorem

Commonly, any fluctuating signal $B(t)$, e.g., $y(t)$, $U(t)$ or $\Phi(t)$ is decomposed into a purely fluctuating contribution $b(t)$ and a mean value $\overline{B(t)}$ as follows

$$B(t) = b(t) + \overline{B(t)} \tag{7.1.20}$$

Consider the *autocorrelation function* of the signal fluctuations defined by

$$\boxed{R_b(\tau) \equiv \overline{b(t+\tau)b(t)} = \lim_{T\to\infty} \frac{1}{2T} \int_{-T}^{T} b(t+\tau)b(t)dt} \tag{7.1.21}$$

which multiplies the signal fluctuations $b(t)$ at the instant t with the signal fluctuation $b(t+\tau)$ at the instant $t+\tau$ and takes the mean over all epochs. If the fluctuations were totally uncorrected, the time-averaged product $\overline{b(t+\tau)b(t)}$ would cancel for any τ . For stationary processes the autocorrelation function must be an even function since $R_b(-\tau) = R_b(\tau)$ holds. Comparing the definition of the autocorrelation function (7.1.21) for $\tau = 0$ and the right-hand side of (7.1.11) for a purely fluctuating quantity (i.e. for $\langle B\rangle^2 = 0$) the value of the autocorrelation function for $\tau = 0$ represents the *variance* of the signal fluctuations

$$\boxed{R_b(\tau = 0) = \sigma_b^2} \tag{7.1.22}$$

For very large times τ one may assume that the power fluctuations are not correlated and the autocorrelation function approaches zero for $\tau \to \infty$. It has been shown in the previous chapter that the Fourier transform of a temporal varying amplitude function represents the amplitude spectrum in the Fourier frequency domain. In the case of the statistically fluctuating power of the oscillator the time function $U(t)$ is not known but the autocorrelation function $R_b(\tau)$ might have been determined. To perform the integration in (7.1.21) we consider $b(t)$ as the Fourier transform $b(t) = F(a(\omega))$ of a quantity $\alpha(\omega)$ whose relevance will become clear later and obtain

$$\begin{aligned} R_b(\tau) &= \lim_{T\to\infty} \frac{1}{2T} \int_{-T}^{T} \frac{1}{(2\pi)^2} \int_{-\infty}^{\infty} a(\omega) e^{i(\omega t+\tau)} \int_{-\infty}^{\infty} a(\omega') e^{i\omega' t} d\omega' dt \\ &= \frac{1}{(2\pi)^2} \int_{-\infty}^{\infty} \int_{-\infty}^{\infty} \left[\lim_{T\to\infty} \frac{1}{2T} \int_{-T}^{T} e^{i(\omega t+t')dt} \right] a(\omega)a(\omega') e^{i\omega\tau} d\omega' d\omega \end{aligned} \tag{7.1.23}$$

after we have interchanged the orders of integration. In the limit $T \to \infty$the term in square brackets can be expressed by the Dirac delta function and, hence,

$$\begin{aligned} R_b(\tau) &= \frac{1}{2\pi} \int_{-\infty}^{\infty} \int_{-\infty}^{\infty} a(\omega)a(\omega') e^{i\omega\tau} \delta(\omega+\omega') d\omega d\omega' \\ &= \int_{-\infty}^{\infty} \frac{|a(\omega)a(\omega')|}{2\pi} e^{i\omega\tau} d\omega \\ &\equiv \int_{-\infty}^{\infty} S_b(f) e^{i2\pi f\tau} df \end{aligned} \tag{7.1.24}$$

To find the significance of $S_b(f)$ we set $\tau = 0$ in (7.1.24) and obtain

$$R_b(0) = \int_{-\infty}^{\infty} S_b(f) df \tag{7.1.25}$$

Recalling that the left-hand side of (7.1.25) is the averaged square of the fluctuating quantity $b(t)$ (see (7.1.21)), S_b represents a power spectral density. In the case of a fluctuating voltage the spectral density is given in units of V^2/Hz.

The autocorrelation function $R_b(\tau)$ and the spectral density function $S_b(f)$ form a Fourier transform pair

$$S_b^{2-\text{sided}}(f) \equiv \mathcal{F}^*\{R_b(\tau)\} = \int_{-\infty}^{\infty} R_b(\tau) e^{-i2\pi f\tau} d\tau \tag{7.1.26}$$

$$R_b(\tau) \equiv \mathcal{F}\{S_b^{2-\text{sided}}(f)\} = \int_{-\infty}^{\infty} S_b(f) e^{i2\pi f\tau} df \tag{7.1.27}$$

where the meaning of the index 2-sided will be discussed below. (7.1.26) is one form of the so-called *Wiener-Khintchine theorem* and allows one to determine the spectral density function from the autocorrelation function of the time-dependent signal amplitude.

If one chooses the power fluctuations $\delta P(t)$ of the oscillator rather than the amplitude fluctuations $b(t)$, the Fourier transformation of the corresponding autocorrelation function $R_{\delta P}(\tau)$ leads to a spectral density of the square of the power fluctuations (in units of W^2/Hz) [7]

Similarly, the fluctuations of the phase $\phi(t)$ with time[8] result in a power spectral density of phase fluctuations in units of rad^2/Hz. Caution is necessary as sometimes in the literature also the square root of $S_b(f) \propto a(\omega)$ (see (7.1.24)) is used.

The power spectral density of the frequency fluctuations in the Fourier domain represented by (7.1.26) is defined for Fourier frequencies $-\infty < f < \infty$ thereby extending to both the positive and negative side of the frequency spectrum. Consequently, $S_b(f)$ is referred to as the two-sided power spectral density $S_b^{2-\text{sided}}(f)$. From $R_b(\tau) = R_b(-\tau)$ it follows that $S_b(f)$ is a real, non-negative and even function, i.e. $S_b(-f) = S_b(f)$. In experimental work, however, only positive frequencies are of interest. Hence, a one-sided power spectral density is often introduced for Fourier frequencies $0 \leq f < \infty$ (see Fig. 7.6) with

$$S_b^{1-\text{sided}}(f) = 2S_b^{2-\text{sided}}(f) \tag{7.1.29}$$

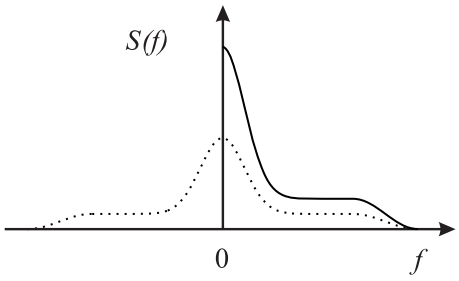

Figure 7.6: Two-sided (dots) and one-sided (line) power spectral densities.

As the power spectral density is a real quantity, it suffices to use a real Fourier transform pair rather than (7.1.26) and (7.1.27). Changing also the limits of the integrals the Wiener- Khintchine relations for a one-sided spectral density function $S_b^{1-\text{sided}}(f)$ are written as

$$S_b^{1-\text{sided}}(f) = 4\int_0^{\infty} R_b(\tau)\cos(2\pi f\tau) d\tau \tag{7.1.30}$$

$$R_b(\tau) = \int_0^{\infty} S_b^{1-\text{sided}}(f)\cos(2\pi f\tau) df \tag{7.1.31}$$

[7] This quantity is closely related to the so-called "Relative Intensity Noise" (RIN)

$$\boxed{\text{RIN}(f) \equiv \frac{S_{\delta p}}{P_0^2}} \tag{7.1.28}$$

often used to describe the power fluctuations of lasers oscillators.

[8] Power spectral densities are used not only to describe fluctuations of a physical quantity with time but also, e.g., to characterize the roughness of a technical surface

7.1.7 Fourier-domain Description of Frequency Fluctuations

For a reasonable frequency-stable oscillator, the instantaneous frequency $\nu(t)$ as function of time can be expected to deviate only slightly from the temporal mean $\overline{\nu}$ and

$$\Delta\nu(t) \equiv \nu(t) - \overline{\nu} \ll \overline{\nu} \tag{7.1.32}$$

holds.

We assume that the frequency excursions $\Delta\nu(t)$ are stationary distributed, i.e., that their distribution is time independent. Similarly as in (7.1.21), we define the autocorrelation function of the frequency deviations

$$\boxed{R_\nu(\tau) = \lim_{T\to\infty} \frac{1}{2T} \int_{-T}^{T} \Delta\nu(t+\tau)\Delta\nu(t)dt} \tag{7.1.33}$$

as a measure of this distribution and use the Wiener-Khintchine relationship to obtain the power spectral density of the frequency deviations from the autocorrelation of the frequency deviations

$$\boxed{S_b^{2-\text{sided}}(f) = \int_{-\infty}^{\infty} R_\nu(\tau) e^{-i2\pi f\tau} d\tau} \tag{7.1.34}$$

Besides the power spectral density of the frequency fluctuations $S_\nu(f)$ the power spectral density $S_y(f)$ of the fractional frequency fluctuations $y(t)$ (see (7.1.19), (7.1.33) and (7.1.34)) can be found as

$$S_y(f) = \frac{1}{\nu_0^2} S_\nu(f) \tag{7.1.35}$$

Similarly one defines a power spectral density of phase fluctuations $S_\phi(f)$ and, by taking into account that the frequency fluctuations are essentially the time derivative of the phase fluctuations ($2\pi\Delta\nu(t) = d/dt\Delta\phi(t)$), one obtains by comparison with (7.1.33) and (7.1.34)

$$S_\nu(f) = f^2 S_\phi(f) \tag{7.1.36}$$

From the last two equations it follows that

$$S_y(f) = (\frac{f}{\nu_0})^2 S_\phi(f) \tag{7.1.37}$$

Each of the defined three power spectral densities contains the same information.

In the typical power spectral density of Fig. 7.7 one can identify different regimes. The delta function at $f = 0$ occurs if $B(t)$ has a non-vanishing mean value $\overline{B}(t)$ and does not show up for a purely fluctuating quantity $b(t)$. The contributions at low Fourier frequencies decreasing with increasing frequency are termed $1/f$-noise. In an intermediate regime the power spectral density of the frequency fluctuations is often independent of the frequency referred to as white frequency noise. The total power contained in the frequency fluctuations is obtained from

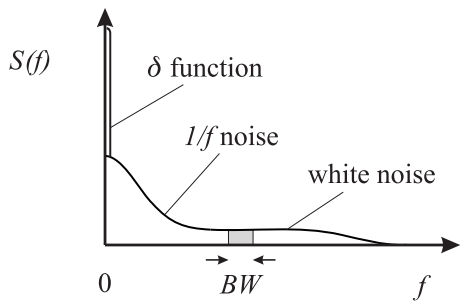

Figure 7.7: Different regimes in a power spectral density. BW: band width.

$$\int_0^\infty S_\nu^{1-\text{sided}}(f)df = \int_{-\infty}^\infty S_\nu^{2-\text{sided}}(f)df = \langle[\Delta\nu(t)]^2\rangle = \sigma_\nu^2 \tag{7.1.38}$$

where we have made use of (7.1.22) and (7.1.25). From reasons of energy conservation this total power must be finite and one therefore expects that for higher frequencies the power spectral density of the frequency fluctuations decreases again (Fig. 7.7).

The determinations of spectral densities of different frequency sources reaching from quartz oscillators to atomic frequency standards has shown that the observed spectral density $S_y(f)$ can be reasonably well modeled by a superposition of five independent noise processes obeying power laws with integer exponents $-2 \leq \alpha \leq 2$

$$S_y(f) = \sum_{\alpha=-2}^{2} h_\alpha f^\alpha \tag{7.1.39}$$

(see Table 7.1). The particular contributions also have characteristic appearances in the time domain (Fig. 7.8).

Table 7.1: Model of a power law of the power spectral density of fractional frequency fluctuations $S_y(f) = h_\alpha f^\alpha$ and the corresponding power spectral density of phase fluctuations $S_\phi(f)$.

$S_y(f)$	$S_\phi(f)$	Type of noise	$\sigma_y^2(\tau)$
$h_{-2}f^{-2}$	$\nu_0^2 h_{-2}f^{-4}$	Random walk of frequency noise	$(2\pi^2 h_{-2}/3)\tau^{+1}$
$h_{-1}f^{-1}$	$\nu_0^2 h_{-1}f^{-3}$	Flicker frequency noise	$2h_{-1}\ln 2\tau^0$
$h_0 f^0$	$\nu_0^2 h_0 f^{-2}$	White frequency noise (Random walk of phase noise)	$(h_0/2)\tau^{-1}$
$h_1 f$	$\nu_0^2 h_1 f^{-1}$	Flicker phase noise	$h_1[1.038 + 3\ln 2\pi f_h\tau]/(4\pi^2)\tau^{-2}$
$h_2 f^2$	$\nu_0^2 h_2 f^0$	Flicker phase noise	$h_1[3h_2 f_h(4\pi^2)]\tau^{-2}$

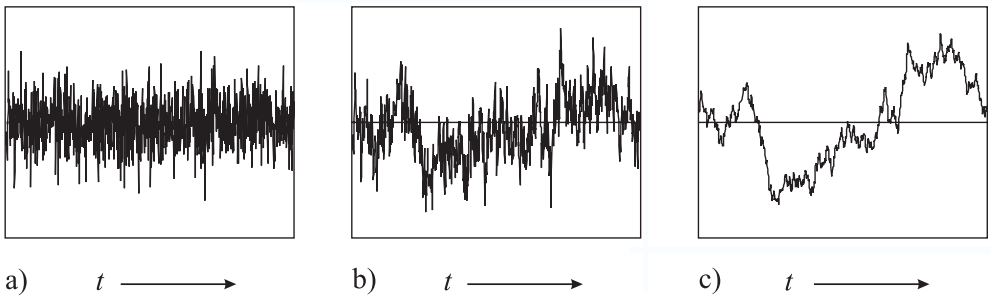

Figure 7.8: Time-domain signal with a) white frequency noise. b) $1/f$ noise. c) $1/f^2$ noise.

In a doubly logarithmic plot the particular contributions to (7.1.39) can be identified readily by their slope, thereby allowing identification of the causes of the noise mechanisms in the oscillators. The particular contributions listed in Table 7.1 can sometimes be identified in frequency standards. The random walk of frequency noise ($\alpha = -2$) is often caused by the influences of environmental parameters, e.g., temperature, vibrations, etc.. Flicker frequency noise ($\alpha = -1$) is observed in active devices such as quartz crystal oscillators, hydrogen masers or laser diodes, but also in passive frequency standards like the Cs clock. White frequency noise ($\alpha = 0$) can result from thermal noise in the oscillator loop of active standards. It is also present in passive standards and may result, e.g., from the shot noise of the photons or atoms where it represents the quantum limit. Flicker phase noise ($\alpha = 1$) often results from contributions of noisy electronics whose level can be reduced by selected components. White phase noise ($\alpha = 2$) becomes important for high Fourier frequencies and can be reduced by band-pass filtering the output of a frequency standard.

One has to keep in mind that the pure power laws of (7.1.39) represent a theoretical model, which is not always observed in this form. The low frequency contributions to the noise sometimes referred to as $1/f$ noise often follow a $f^{-\beta}$ dependence with $0.5 \leq \beta \leq 2$ (see, e.g., Fig. 7.9) where the observed power law may also be due to a superposition of several noise processes.

7.1.8 Power Spectrum of a Source with White Frequency Noise

We now consider a source whose power spectral density in the Fourier-frequency domain can be represented as *white* (frequency independent) frequency noise S_ν^0 (see Table 7.1). Consequently,

$$\boxed{S_\phi(f) = \frac{S_\nu^0}{f^2} = \frac{\nu_0^2 h_0}{f^2}} \tag{7.1.40}$$

holds and the integral in the exponential and can be solved analytically using $\int_0^\infty [1-\cos(bx)]/x^2 dx = \pi|b|/2$ leading to

$$\begin{aligned} S_E(\nu-\nu_0) &= E_0^2 \int_{-\infty}^{\infty} e^{-[i2\pi(\nu-\nu_0\tau)]} \exp\left(-\int_0^\infty S_\phi(f)[1-\cos(2\pi f\tau)]df \right) d\tau \\ &= E_0^2 \int_{-\infty}^{\infty} e^{-[i2\pi(\nu-\nu_0\tau)]} \exp\left(-\pi^2 h_0 \nu_0^2 |\tau|\right) d\tau \\ &= 2E_0^2 \int_0^{\infty} e^{-\tau[i2\pi(\nu-\nu_0)+\pi^2 h_0 \nu_0^2]} d\tau \end{aligned} \tag{7.1.41}$$

Solving the integral (7.1.41) and keeping the real part leads to the power spectral density of

$$\boxed{S_E(\nu-\nu_0) = E_0^2 \frac{h_0\pi^2\nu_0^2}{h_0^2\pi^4\nu_0^4 + 4\pi^2(\nu-\nu_0)^2} = 2E_0^2 \frac{\gamma/2}{(\gamma/2)^2 + 4\pi^2(\nu-\nu_0)^2}} \tag{7.1.42}$$

with $\gamma \equiv 2h_0\pi^2\nu_0^2 = 2\pi(\pi h_0 \nu_0^2) = 2\pi(\pi S_\nu^0)$. Hence, the power spectral density of frequency fluctuations in the carrier-frequency domain of an oscillator with white frequency noise S_ν^0 in the Fourier-frequency domain, is a Lorentzian whose full width at half maximum is given by

$$\boxed{\Delta\nu_{\mathrm{FWHM}} = \pi S_\nu^0} \tag{7.1.43}$$

Similarly, other types of phase noise spectral densities can be calculated accordingly. Godone and Levi have furthermore treated the case of white phase noise and flicker phase noise.

7.1.9 Spectrum of a Diode Laser

As an example of white frequency noise, consider the frequency fluctuations in a laser resulting from the spontaneous emission of photons. They lead to the so-called *Schawlow-Townes* linewidth

$$\boxed{\Delta\nu_{\mathrm{QNL}} = \frac{2\pi h\nu_0 (\Delta\nu_{1/2})^2 \mu}{P}} \tag{7.1.44}$$

where $h\nu_0$ is the photon energy, $\Delta\nu_{1/2}$ is the full width at half maximum of the passive laser resonator, $\mu \equiv N_2/(N_2-N_1)$ is a parameter describing the population inversion in the laser medium, and P is the output power of the laser. This quantum-noise limited power spectral density (which is enhanced for laser diodes by Henrys linewidth enhancement factor) can be found in the measured spectral noise of a solitary diode laser (Fig. 7.9) at Fourier frequencies above a corner frequency of about 80 kHz. At frequencies below the corner frequency the power spectral density increases with a power law of roughly $1/f$. The white frequency noise regime is also visible above the corner frequency f_c of about 200 kHz if the cavity of the diode laser is extended but $S_\nu(f)$ is reduced by about 33 dB according to the reduced linewidth $\Delta\nu_{1/2}$ (see (7.1.44)).

As the $1/f$-like behavior often results from technical noise which is present in any oscillator to some degree it is interesting to investigate the validity of (7.1.42). OMahony and Henning have

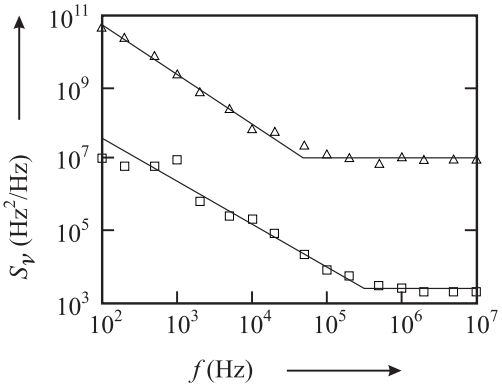

Figure 7.9: Measured power spectral densities of frequency fluctuations versus Fourier frequency f of a diode laser without optical feedback (triangles) and with optical feedback from a grating (squares) after with permission.

investigated the effect of low frequency $(1/f)$ carrier noise on the linewidth of a semiconductor laser. From their findings Koch gives a criterion that allows one to obtain information about the lineshape from the positions of the corner frequencies f_c as follows

$$S_\nu(f_c)/f_c \gg 1 : \Longrightarrow \qquad \text{Lorentzian lineshape} \tag{7.1.45}$$

$$S_\nu(f_c)/f_c \ll 1 : \Longrightarrow \qquad \text{Gaussian lineshape.} \tag{7.1.46}$$

We apply these criteria to the power spectral density of frequency noise displayed in Fig. 7.9 where one finds, for the solitary laser diode (triangles), $S_\nu(f_c)/f_c > 100$ and, hence, criterion (7.1.45) applies. With (7.1.43) one expects a Lorentzian profile of about 5MHz linewidth. From the power spectral density of frequency fluctuations (squares in Fig. 7.9) of another diode laser with extended cavity one finds $S_\nu(f_c)/f_c \approx 10^{-2}$ and hence expects a Gaussian lineshape according to criterion (7.1.46). The origin of the Gaussian lineshape can be thought of as resulting from a small Lorentzian line whose width is given by (7.1.43) which statistically wanders around a central frequency. The width of the Gaussian depends on the time T of averaging, as the measurement time T also defines the lowest measurable Fourier frequency $1/T$. For a true $1/f$ behavior of S_ν the linewidth would be infinite as $\int_{1/T}^{\infty} S_\nu(f)df = \infty$ holds (see (7.1.41)). Experimentally, however, one always finds a finite linewidth resulting from the finite measurement time T with the low-frequency cut off $1/T$.

The mean frequency excursion $\Delta\nu_{\rm rms}$ (linewidth) can be computed as

$$\boxed{\Delta\nu_{\rm rms} = \sqrt{\int_{1/T}^{f_c} S_\nu(f)df}} \tag{7.1.47}$$

from (7.1.38). In the case of the laser with optical feedback in an extended cavity arrangement (squares in Fig. 7.9) one derives a FWHM of the Gaussian of about 120 kHz for a measurement time of 10 ms.

7.2 Amplitude noise: Relaxation oscillations[9]

7.2.1 Introduction

Thus far we have restricted our study of the laser to the case of continuous-wave, single-mode operation . In this chapter we will consider time-dependent, transient effects, including relaxation oscillations and Q switching. We will also extend our single-mode theory somewhat to the case in which several or many cavity modes can oscillate simultaneously . This allows us in particular

[9]Chapter 12 (Page 365 - 370) - Lasers - Peter W. Milonni, Joseph H. Eberly - New York [etc.] : Wiley, cop. 1988

to understand the important technique called mode locking, a way to obtain ultrashort pulses of light.

7.2.2 Rate Equation for Intensities and Populations

In the preceding two chapters we have found it convenient and instructive to describe the strength of the cavity field either in terms of intensity I_ν or photon number q_ν. In the present chapter it will be convenient to use the intensity description. We will therefore begin with a brief review of the appropriate equations coupling the intensity and the laser level population densities N_2 and N_1 .

In general the cavity intensity will vary both in time and space. We will continue in this chapter to make the plane-wave approximation in which the intensity is assumed to be uniform in any plane perpendicular to the cavity axis. Furthermore for the most common situation in which the mirror reflectivities are large (say, $> 50\%$), the cavity intensity is approximately unifom1 along the cavity axis if we ignore the rapidly varying $\sin^2 kz$ interference term. So it is useful again to make the uniform-field approximation, but now to include the time dependence of the cavity intensity. First we recall equation of Intensity-Gain:

$$\begin{aligned}\frac{dI_\nu}{dt} &= \frac{cl}{L}\Big(g(\nu)I_\nu - \frac{1}{2l}(1-r_1r_2)I_\nu\Big)\\ &= \frac{cl}{L}[g(\nu)-g_t]I_\nu \end{aligned} \tag{7.2.1}$$

For simplicity we will assume that the gain cell fills the entire space between the mirrors . Then $l = L$ and

$$\frac{dI_\nu}{dt} = c[g(\nu)-g_t]I_\nu \tag{7.2.2}$$

Recall that $I_\nu = I_\nu^{(+)} + I_\nu^{(-)}$ is the sum of the two traveling-wave intensities; in the case of high mirror reflectivities, the two are approximately equal.

In terms of the cavity intensity we can write the population rate equations

$$\frac{dN_2}{dt} = -\frac{g(\nu)I_\nu}{h\nu} - \Gamma_{21}N_2 + K_2 \tag{7.2.3a}$$

$$\frac{dN_1}{dt} = \frac{g(\nu)I_\nu}{h\nu} + \Gamma_{21}N_2 + K_1 \tag{7.2.3b}$$

where the rates Γ_{21} , K_2 , and K_1 are, again, level decay and pumping rates. Since N_2 and N_1 are populations per unit volume, the pumping rates have units of $(\text{volume})^{-1}$ $(\text{time})^{-1}$. Equations (7.2.2) and (7.2.3) are coupled rate equations for I_ν, N_2, and N_1. The coupling is through the gain coefficient

$$\begin{aligned} g(\nu) &= \frac{\lambda^2 A}{8\pi}(N_2-N_1)S(\nu)\\ &= \sigma(\nu)(N_2-N_1)\end{aligned} \tag{7.2.4}$$

where we assume for simplicity that $g_2/g_1 = 1$.

The population rate equations (7.2.3) are easily modified to suit a particular laser medium. We have already described such modifications in the case of the stylized three- and four-level models. Since we will be describing in this chapter some rather general phenomena that transcend specific inversion schemes, it will be adequate to use the simple rate equations (7.2.3) for the laser level population densities.

For many purposes the rate equations (7.2.2) and (7.2.3) may be simplified somewhat. One simplifying assumption is that $N_1 \ll N_2$, i. e ., that the lower laser level population is negligible compared with the upper laser level population. This would be the case in a four-level laser, where the lower level decays very rapidly compared with the stimulated emission (absorption) rate. Then $g(\nu) = \sigma(\nu)N_2$, and (7.2.3) and (7.2.3a) become

$$\frac{dI_\nu}{dt} = c\sigma(\nu)N_2 I_\nu - cg_t I_\nu \tag{7.2.5a}$$

$$\frac{dN_2}{dt} = -\frac{\sigma(\nu)}{h\nu}N_2 I_\nu - \Gamma_{21}N_2 + K_2 \tag{7.2.5b}$$

7.2.3 Relaxation Oscillation

The coupled equations (7.2.5) for I_ν and N_2 are simple in appearance, but they have no known general solution. However, it is easy to find the *steady-state* solutions which we denote $\overline{I}_\nu$ and N_2 These are obtained simply by replacing the left sides of (7.2.5) by zero and solving the resulting algebraic equations, with the result

$$\overline{I}_\nu = h\nu\Big(\frac{K_2}{g_2} - \frac{\Gamma_{21}}{\sigma(\nu)}\Big) \tag{7.2.6a}$$

$$\overline{N}_2 = \frac{g_t}{\sigma(\nu)} \tag{7.2.6b}$$

These solutions may also b written in a different form to show explicitly how $\overline{N}_2$ saturates with increasing I_ν.

It is possible to solve these equations approximately if the laser is operating very near to steady state. In this case we write

$$I_\nu = \overline{I}_\nu + \epsilon \tag{7.2.7a}$$

$$N_2 = \overline{N}_2 + \eta \tag{7.2.7b}$$

and assume

$$|\epsilon| \ll \overline{I}_\nu \tag{7.2.8a}$$

$$|\eta| \ll \overline{N}_2 \tag{7.2.8b}$$

This approximation allows the equations (7.2.5) to be linearized and solved, as follows.

Using (7.2.7) in (7.2.5a), we have

$$\frac{d}{dt}(\overline{I}_\nu + \epsilon) = c\sigma(\overline{N}_2 + \eta)(\overline{I}_{\nu+\epsilon}) - cg_t(\overline{I}_\nu + \epsilon) \tag{7.2.9}$$

which is the same (since $d\overline{I}_\nu/dt = 0$) as

$$\begin{aligned}\frac{d\epsilon}{dt} &= c\sigma(\overline{N}_2 + \eta)(\overline{I}_\nu + \epsilon) - cg_t(\overline{I}_\nu + \epsilon) \\ &= c\sigma(\overline{N}_2\overline{I}_\nu + \overline{N}_2\epsilon + \overline{I}_\nu\eta + \eta\epsilon) - cg_t(\overline{I}_\nu + \epsilon)\end{aligned} \tag{7.2.10}$$

Now $\overline{I}_\nu$ and $\overline{N}_2$ are such as to make the right sides of (7.2.5) vanish. In particular

$$c\sigma\overline{N}_2\overline{I}_\nu - cg_t\overline{I}_\nu = 0 \tag{7.2.11}$$

Using this relation in (7.2.10), we obtain the much simpler equation

$$\frac{d\epsilon}{dt} = c\sigma\eta\overline{I}_\nu + c\sigma\eta\epsilon \tag{7.2.12}$$

This is still nonlinear (because of the term $\eta\epsilon$) , but now the nonlinearity is very small because it involves the product of the small quantities η and ϵ. Near enough to steady state [recall (7.2.8)], such second-order-small terms can be dropped altogether without significant error. Thus we obtain the following linear equation for the time dependence of the departure of the cavity intensity from its steady state value:

$$\frac{d\epsilon}{dt} = (c\sigma\overline{I}_\nu)\eta \tag{7.2.13}$$

where the factor in parentheses is constant in time.

The same procedure can be applied to (7.2.5b). Again the product $\eta\epsilon$ is very small and can be dropped, and again the definitions of $\overline{I}_\nu$ and $\overline{N}_2$ can be used to cancel some terms. The result is

$$\frac{d\eta}{dt} = -\frac{g_t}{h\nu}\epsilon - \frac{\sigma K_2}{g_t}\eta \tag{7.2.14}$$

Equations (7.2.13) and (7.2.14) are still coupled to each other, but they are now linear and easily solved . We use (7.2.13) to replace η in (7.2.14) by $(c\sigma\overline{I}_\nu)^{-1}\, d\epsilon/dt$ to get

$$\frac{d^2\epsilon}{dt^2} + \gamma\frac{d\epsilon}{dt} + \omega_0^2\epsilon = 0 \tag{7.2.15}$$

where we define

$$\gamma = \sigma K_2/g_t \tag{7.2.16}$$

and

$$\omega_0^2 = \frac{c\sigma g_t}{h\nu}\overline{I}_\nu \tag{7.2.17}$$

The solution to (7.2.15) is easily found to be

$$\epsilon(t) = Ae^{-\gamma t/2}\cos(\omega t + \phi) \tag{7.2.18}$$

where A and ϕ are the initial amplitude and phase of $\epsilon(t)$, and the frequency of oscillation is given by

$$\omega = \sqrt{\omega_0^2 - \frac{\gamma^2}{4}} \tag{7.2.19}$$

For definiteness we assume $\omega > \gamma/2$, making ω real. Thus, near to the steady state, the cavity intensity oscillates about the steady-state value $\overline{I}_\nu$, and gradually approaches $\overline{I}_\nu$ at the (exponential) rate $\gamma/2$:

$$I_\nu = \overline{I}_\nu + Ae^{-\gamma t/2}\cos(\omega t + \phi) \tag{7.2.20}$$

This is called a *relaxation oscillation.* Similar behavior is observed in a wide variety of nonlinear systems.

Although the relaxation-oscillation solution (7.2.18) is valid only if $|\epsilon| \ll \overline{I}_\nu$ [recall (7.2.3)], the nature of the solution is of general importance. The critical feature oj the solution is that γ is positive . This guarantees that the steady-state solution $\overline{I}_\nu$ is a *stable* solution. That is , if some outside agent slightly disturbs the laser while it is running in steady state, the effect of the disturbance decays to zero, thus returning the laser to steady state again. If γ were negative, a small disturbance would grow , and the steady state would therefore be unstable, and thus of very little practical significance.

We may write the period T_r and lifetime τ_r of the relaxation oscillations as

$$\boxed{T_r = \frac{2\pi}{\omega_0} = \frac{2\pi}{\sqrt{(c/\tau_{21})(g_0 - g_t)}}} \tag{7.2.21}$$

and

$$\tau_r = \frac{1}{\gamma} = \frac{g_t}{g_0}\tau_{21} \tag{7.2.22}$$

where go is the small -signal gain and $\tau_{21} = \Gamma_{21}^{-1}$ is the lifetime of the upper laser level. From (7.2.22) or (7.2.16) we see that the duration of the relaxation oscillations decreases with increasing pumping rate K_2 of the gain medium. Likewise the period T_r. of the relaxation oscillations should decrease with increased g_0. These predicted trends are consistent with many experimental observations.

It is possible to observe relaxation oscillations in the output intensity of a laser after it is turned on and approaches a steady-state operation. Perturbations in the pumping power can also cause relaxation oscillations to appear spontaneously. In some cases, especially in solid-state lasers, the relaxation time τ_r may be relatively large, making relaxation oscillations readily apparent on an oscilloscope trace of the laser output intensity.

Example: T_r and τ_r in Ruby laser

As an example, consider a ruby laser with mirror reflectivities $r_1 \approx 1.0$, $r_2 \approx 0.94$, and a ruby rod of length $l = 5.0$ cm. For such a laser $g_t \approx (1/2l)(1 - r_2) = 0.006$ cm^{-1}, so that $cg_t \approx 1.8 \times 10^8$ sec $^{-1}$. For ruby the upper level lifetime $\tau_{21} \approx 2 \times 10^{-3}$ sec. Assuming a pumping level such that $g_0/g_t = 2.0$, we compute from (7.2.21) and (7.2.22) the period and lifetime of relaxation oscillations:

$$T_r \approx 21\mu\text{sec} \tag{7.2.23}$$

$$\tau_r \approx 2 \text{ msec} \tag{7.2.24}$$

Relaxation-oscillation periods are often in the microsecond range, as in this example. The damping time τ_r is particularly large in ruby because of its unusually long upper-level lifetime τ_{21} . Relaxation oscillations are therefore particularly pronounced in ruby. The output of a continuously pumped ruby laser typically consists of a series of irregular spikes, and this spiking behavior is usually attributed to relaxation oscillations being continuously excited by various mechanical and thermal perturbations.

7.3 Direct-Current Modulation of Semiconductor Lasers[10]

Since the main application of semiconductor lasers is as sources for optical communication systems, the problem of high-speed modulation of their output by the high-data-rate information is one of great technological importance.

A unique feature of semiconductor lasers is that, unlike other lasers that are modulated externally , the semiconductor laser can be modulated directly by modulating the excitation current. This is especially important in view of the possibility of monolithic integration of the laser and the modulation electronic circuit.

If we denote the photon density inside the active region of a semiconductor laser by P and the injected electron (and hole) density by N, then we can write

$$\begin{aligned} \frac{dN}{dt} &= \frac{I}{eV} - \frac{N}{\tau} - A(N - N_{tr})P \\ \frac{dP}{dt} &= A(N - N_{tr})P\Gamma_a - \frac{P}{\tau_p} \end{aligned} \tag{7.3.1}$$

where I is the total current, V the volume of the active region, τ the spontaneous recombination lifetime, τ_p the photon lifetime as limited by absorption in the ing media, scattering and coupling through the output mirrors.

The term $A(N - N_{tr})P$ is the net rate per unit volume of induced transitions. N_{tr} is the inversion density needed to achieve transparency, and A is a temporal growth constant that by definition is related to the constant B defined by the relation $A = Bc/n$. Γ_a is the filling factor defined by (15 3-3) in Chapter 15.3 Yariv, Optical Electronics in Modern Communications and Its presence here is to ensure that the total number, rather than the density variable used in (7.3.1), of electrons undergoing stimulated transitions is equal to the number of photons emitted. The contribution of spontaneous emission to the photon density is neglected since only a very small fraction (10^{-4}) on the spontaneously emitted power enters the lasing mode.

By setting the left side of (7.3.1) equal to zero, we obtain the steady-state solution N_0 and P_0

$$\begin{aligned} 0 &= \frac{I_0}{eV} - \frac{N_0}{\tau} - A(N_0 - N_{tr})P_0 \\ 0 &= A(N_0 - N_{tr})P_0\Gamma_a - \frac{P_0}{\tau_p} \end{aligned} \tag{7.3.2}$$

[10]Chapter 15 (Page 582 - 587) - Optical Electronics in Modern Communications- Fifth Edition - Amnon Yariv - Oxford University Press, 1997

We consider the case where the current is made up of dc and ac components

$$I = I_0 + i_1 e^{i\omega_m t} \tag{7.3.3}$$

and define the small-signal modulation response n_1 and P_1 by

$$N = N_0 + n_1 e^{i\omega_m t} \qquad P = P_0 + p_1 e^{i\omega_m t} \tag{7.3.4}$$

where N_0 and P_0 are the dc solutions of (7.3.2).

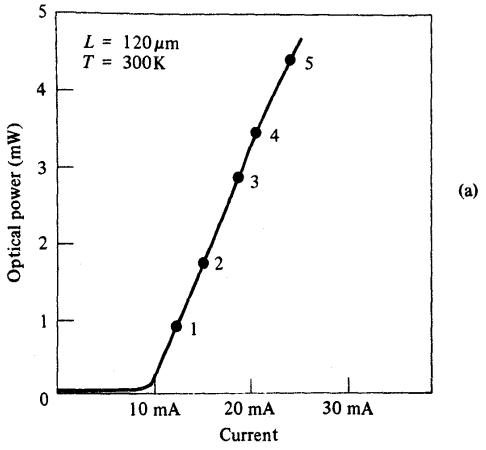

Figure 7.10: (a) *CW* light output power versus current characteristic of a laser of length = 120 μm.

Using (7.3.3), (7.3.4), and the result $A(N_0 - N_{tr}) = (\tau_p \Gamma_a)^{-1}$ from (7.3.2) In (7.3.1) leads to the small-SIgnal algebraic equations

$$\begin{aligned} -i\omega_m n_1 &= -\frac{I_1}{eV} + \Big(\frac{1}{\tau} + AP_0\Big) n_1 + \frac{1}{\tau_p \Gamma_a} p_1 \\ i\omega_m p_1 &= AP_0 \Gamma_a n_1 \end{aligned} \tag{7.3.5}$$

Our main interest is in the modulation response $p_1(\omega_m)/i_1(\omega_m)$ so that from (7.3.5) we obtaIn

$$p_1(\omega_m) = \frac{-(i_1/eV) AP_0 \Gamma_a}{\omega_m^2 - i\omega_m/\tau - i\omega_m AP_0 - AP_0/\tau_p} \tag{7.3.6}$$

A typical measurement of $P_1(\omega_m)$ is shown in Figure 7.10(b). The response curve is at at small frequencies, peaks at the "relaxation resonance frequency" ω_R, and then drops steeply. The expression for the peak frequency is obtained by minimizing the magnitude of the denominator of (7.3.6)

$$\omega_R = \sqrt{\frac{AP_0}{\tau_p} - \frac{1}{2}\Big(\frac{1}{\tau} + AP_0\Big)^2} \tag{7.3.7}$$

In a typical semiconductor laser with $L = 300$ μm, we have $\tau_p \approx (nlc)(\alpha - (1/L)\ln R)^{-1}$ 10^{-12} s, τ 4×10^{-9} s, and AP_0 10^9 s^{-1} so that to a very good accuracy

$$\omega_R = \sqrt{\frac{AP_0}{\tau_p}} \tag{7.3.8}$$

The last result is extremely useful, since it suggests that to increase ω_R and thus increase the useful linear region of the modulation response $p_1(\omega_m)/i_1(\omega_m)$, we need to increase the optical gain coefficient A, decrease the photon lifetime τ_p, and operate the laser at as high internal photon density P_0 as possIble. The observed linear dependence of the modulation resonance frequency ω_R on the square .root of the power output $p\sqrt{P}$ is demonstrated in Figure 7.11(c) for lasers of varying

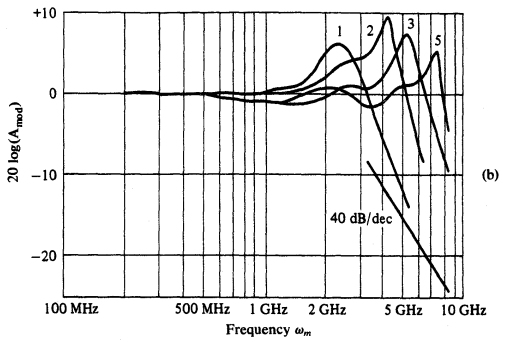

Figure 7.11: (b) Modulation characteristics of this laser at various bias points indicated in the plot.

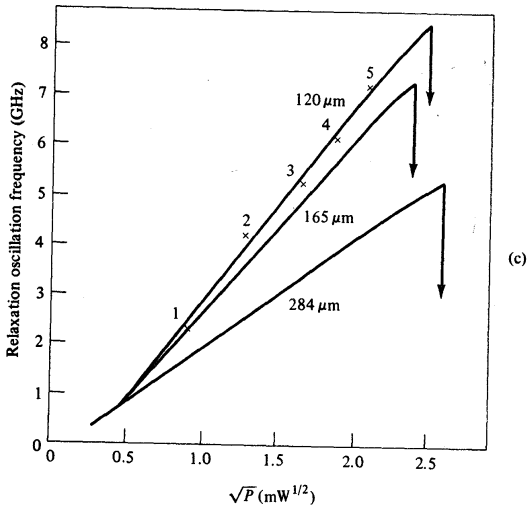

Figure 7.12: (c) Measured relaxation oscillation resonance frequency of lasers of various cavity lengths as a function of $\sqrt{P}$, where P is the cw output optical power. The points of catastrophic damage are indicated by downward pointing arrows.

lengths. A detailed discussion of the optimum strategy for maximizing ω_r is given in Reference. Figure 7.12(d) shows the microwave current feeding electrodes for high-frequency modulation, and 7.13(e) the corresponding frequency response.

It is somewhat tedious but straightforward to show that (7.3.7) can also be written as

$$\omega_r = \sqrt{\frac{1 + A\tau_p \Gamma_a N_{tr}}{\tau \tau_p} \left(\frac{I_0}{I_{th}} - 1 \right)} \tag{7.3.9}$$

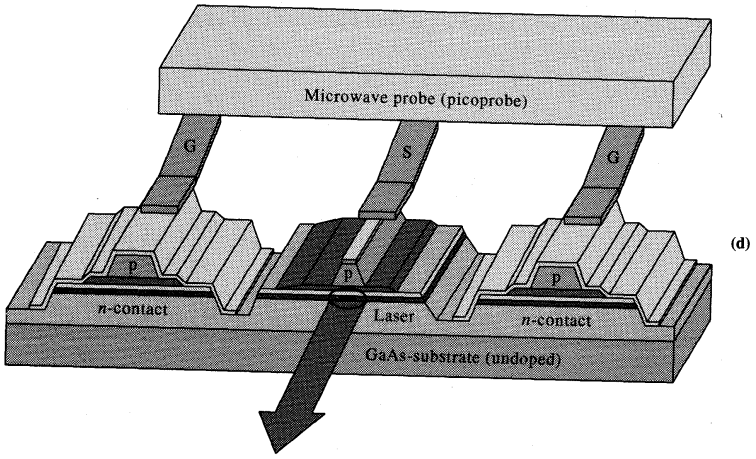

Figure 7.13: (d) Current feed network for microwave modulation of high-speed lasers.